

Shake table testing and numerical simulation of a self-centering energy dissipative braced frame

Jeffrey Erochko¹, Constantin Christopoulos^{2,*†}, Robert Tremblay³ and Hyung-Joon Kim⁴

¹Department of Civil and Environmental Engineering, University of Toronto, Carleton University, Ottawa, ON, Canada
formerly, Department of Civil Engineering, University of Toronto

²Department of Civil Engineering, University of Toronto, Toronto, ON, Canada

³Department of Civil, Geological and Mining Engineering, École Polytechnique, Montréal, QC, Canada

⁴Department of Architectural Engineering, University of Seoul, Seoul, South Korea

SUMMARY

The self-centering energy dissipative (SCED) brace is a new steel bracing member that provides both damping to the structure and a re-centering capability. The goal of this study was to confirm the behavior of SCED braces within complete structural systems and to confirm the ability to model these systems with both a state-of-the-art computer model as well as a simplified model that would be useful to practicing engineers. To these ends, a three-story SCED-braced frame was designed and constructed for testing on a shake table. Two concurrent computer models of the entire frame were constructed: one using the OPENSEES nonlinear dynamic modeling software, and a simplified model using the commercial structural analysis software SAP2000. The frame specimen was subjected to 12 significant earthquakes without any adjustment or modification between the tests. The SCED braces prevented residual drifts in the frame, as designed, and did not show any significant degradation due to wear. Both numerical models were able to predict the drifts, story shears, and column forces well. Peak story accelerations were overestimated in the models; this effect was found to be caused by the absence of transitions at stiffness changes in the hysteretic model of the braces. Copyright © 2013 John Wiley & Sons, Ltd.

Received 17 April 2012; Revised 23 January 2013; Accepted 29 January 2013

KEY WORDS: residual drifts; steel frames; shaking table testing; nonlinear analysis; high performance systems

1. INTRODUCTION

The current state-of-the-art for the design of building structures to resist earthquake loading typically incorporates the use of well detailed inelastic mechanisms (or structural ‘fuses’). Some examples of inelastic mechanisms include buckling/yielding steel braces, buckling-restrained braces, steel, or concrete moment frames, and concrete walls. The load reduction and limitation benefits that are provided by these mechanisms are typically achieved at the cost of localized damage in the inelastic mechanism itself. The remainder of the structure is then designed according to the principles of capacity design to restrict damage to those elements only.

This design paradigm has been a significant step forward in seismic design philosophy, but still suffers from two notable drawbacks. First, buildings with typical inelastic elements are likely to sustain residual deformations after a significant seismic event. Previous studies have recognized the importance of residual drift as a key performance index for building design [1, 2]. A recent analytical study has suggested that the

*Correspondence to: Constantin Christopoulos, Department of Civil Engineering, University of Toronto, 35 St. George Street, Toronto, ON M5S 1A4, Canada.

†E-mail: c.christopoulos@utoronto.ca

likely magnitude of this drift may be estimated by subtracting the yield drift from the maximum expected drift, especially for taller buildings [3]. Another recent study suggested that a residual drift $>0.5\%$ means that it will likely be less expensive to completely replace a building than to retrofit it [4]. The second drawback is that for earthquakes with any significant duration, typical inelastic systems tend to suffer from a progressive collapse mechanism. This problem arises because drifts in these systems tend to accumulate in one direction due to a bias that is created in the direction of the inelastic lean. Under the influence of P-Delta effects, successive cycles tend to pull the building predominantly in this same direction, eventually leading to collapse [5].

Self-centering systems arose primarily to mitigate the consequences of residual drifts, in an effort to develop building systems that can satisfy more stringent performance levels under earthquake loads. The common feature of all self-centering systems is that, unlike typical yielding or friction elements in buildings that exhibit a parallelogram-shaped response, self-centering systems exhibit a flag-shaped hysteretic response similar to that shown in Figure 1.

A number of different practical structural configurations have been devised that are able to produce global self-centering behavior. Notably, these include self-centering moment-resisting frames [6–11] and rocking wall systems [6, 12–16]. In Canada, the self-centering energy dissipative (SCED) brace has been developed to produce a full flag-shaped response within an easily erected bracing member that is scalable to force levels that are similar to the forces that may be achieved by steel yielding systems [17].

1.1. The self-centering energy dissipative brace

A schematic representation of the mechanism and behavior of the SCED brace is shown in Figure 1. The brace mechanism consists of four main elements: (i) an inner member (usually an I-beam section or a steel tube), (ii) an outer member (usually a steel tube), (iii) an energy dissipating device that activates on the basis of the relative movement of the inner and outer sections, and (iv) a set of tendons that are pre-tensioned and clamp both the inner and outer members at both ends via a pair of free end plates. The inner member is connected at one end of the brace, and the outer member is connected at the other end of the brace. The flag-shaped hysteretic behavior is achieved through the interaction of these four elements as shown in Figure 1. The tendons are pre-tensioned during assembly and, therefore, provide a restoring force that constantly pulls all of the elements back to their initial positions. The energy

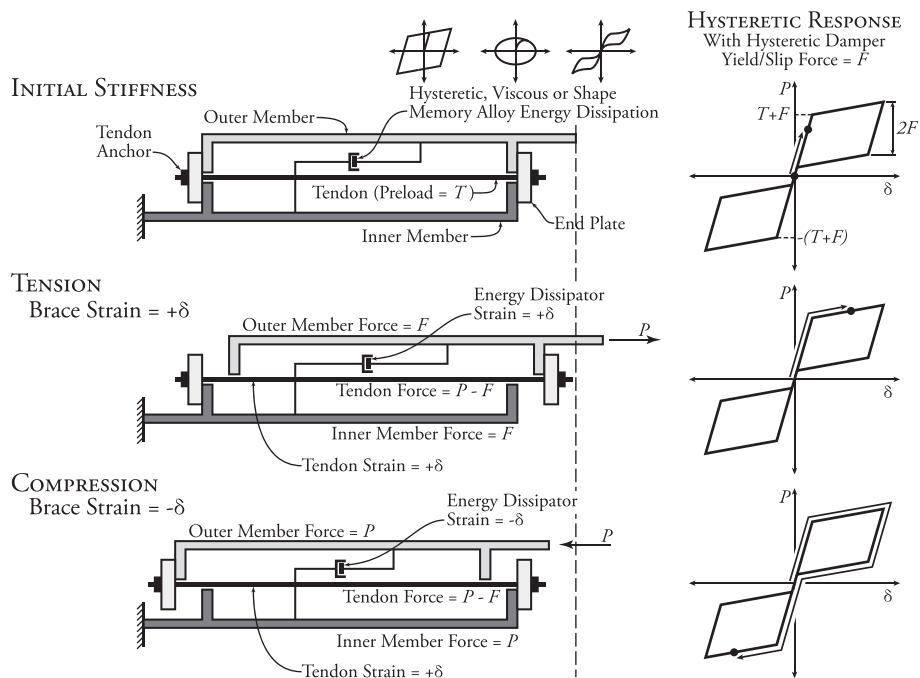


Figure 1. Self-centering energy dissipative brace mechanics.

dissipating device provides the width of the flag that is equal to $2F$ (Figure 1). For the brace to be fully self-centering, the only criterion is that the pretension in the tendons (T) must be greater than the activation/yield force for the energy dissipater (F).

The SCED brace has previously been tested as a prototype both axially and within a single-story frame under dynamic, displacement-driven inter story loading [17]; however, prior to this study, there had been no true base-acceleration-driven dynamic evaluation of a full multi-story structural system incorporating SCED braces. This paper presents a shaking table study that was conducted on a one-third scale, three-story SCED-braced frame. The two primary goals of the study were as follows: (i) to evaluate the dynamic response of a multi-story SCED frame system subjected to multiple types of ground motions from different seismic environments, and (ii) to assess the ability of computer models of differing complexity, including commercial software that is widely used in practice, to accurately predict the seismic response of a multi-story SCED-braced frame.

Additionally, a previous numerical study has found that models of SCED-braced frames experience high peak accelerations when experiencing high-velocity stiffness transitions, and it was posited in that study that this effect is caused by the time lag between activation of SCED braces in adjacent floors and sharp transitions between the elastic and inelastic stiffness in the brace hysteresis model [18]. The current study will examine the acceleration response of the real SCED-braced frame with the aim of determining the cause of these high accelerations.

2. BUILDING DESIGN AND PROPERTIES

2.1. Location and prototype design according to ASCE-7

The full design of the prototype building may be found in the work of Kim [19], and the results of this design are summarized in the later text. The prototype building is a three-story steel office building located on a Class D site in Los Angeles, California. The building was designed and detailed according to ASCE 7-05 [20], AISC 360-05 [21], and AISC 341-05 [22]. The building has three bays in the N–S direction totalling 27.43 m in length and six bays in the E–W direction totalling 36.58 m in length (Figure 2). For the lateral load-resisting system, it uses four perimeter SCED-braced frames in the N–S

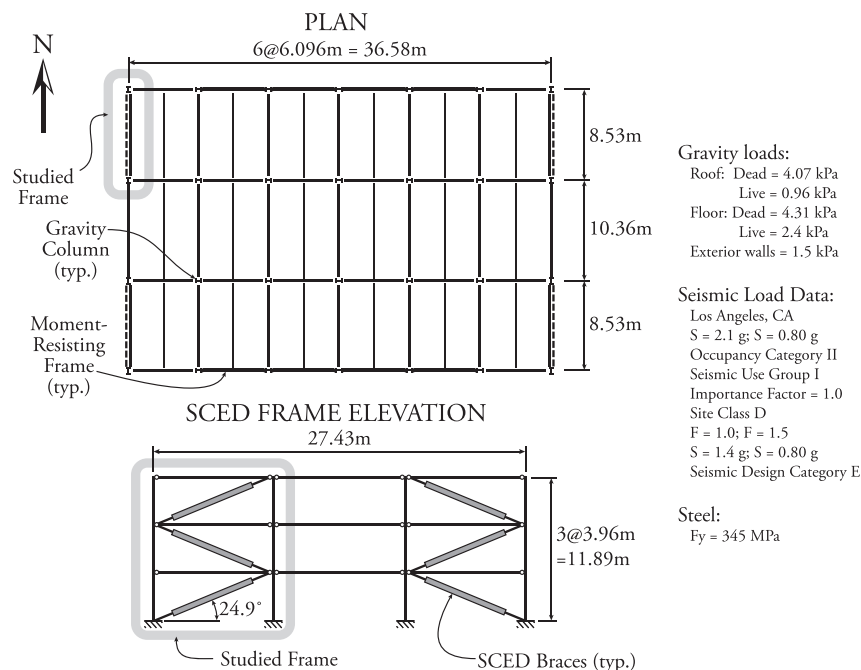


Figure 2. Prototype building design.

direction and two four-bay perimeter moment-resisting frames in the E–W direction. The total seismic weight for the building is 12732 kN. Additional design loads and seismic data are shown in Figure 2.

Because previous studies have shown that SCED-braced frames have seismic drift and force demands similar to buckling-restrained braces [18, 23, 24], the SCED-braced frames were designed using the same seismic design parameters given for buckling-restrained braces in ASCE 7-05 [22]: $R = 7.0$, $C_d = 5.5$, and $\Omega_0 = 2.0$. The moment-resisting frames were designed using the seismic design parameters for special steel moment-resisting frames: $R = 8.0$, $C_d = 5.5$, and $\Omega_0 = 3.0$.

Both of the lateral force-resisting systems were designed using the Equivalent Lateral Force method in ASCE 7. For the SCED-braced frame direction, the design period T was taken as 0.44 s ($T = C_u T_a$, with $C_u = 1.4$, and $T_a = 0.0488 \times 11.887^{0.75} = 0.31$ s). This resulted in a seismic base shear of $0.2W = 2546$ kN. In-plane torsion was omitted for simplicity. Therefore, the base shear for a single-braced frame was equal to 637 kN.

The resulting SCED brace properties for each story of the studied frame are shown in Table I. In this table, the target SCED values were determined by projecting the story shear force into the diagonal direction and then dividing by a resistance factor of 0.9. The selected SCED properties shown in the table (the rightmost four columns) are the result of full scale, realistic SCED brace designs that were conducted to meet the target values. At one of their ends, the braces are connected to the frame members with friction bolted connections acting as external fuses [17]. These external end fuses are designed to activate at a story drift angle of 2% to accommodate story drifts up to 4% without structural damage. The resulting section properties for the other members in the SCED-braced frame are not shown, but may be found in the work of Kim [19].

2.2. Scaling of the prototype design for the shake table

Following the prototype building design, one of the SCED-braced frames in the building was scaled down (one-third scale) to meet the physical limitations of the shaking table at École Polytechnique in Montreal. This process resulted in scaling factors of 0.333 for length, 1.000 for acceleration, stresses and elastic modulus, and 0.577 for time, 0.111 for area, force and mass.

Note that this particular scaling regime resulted in a time compression, but left the accelerations untouched. The scaling factor for forces (1/9) resulted in a reduced total building seismic weight of 1415 and 354 kN for a single SCED braced frame. Using the same proportion, the base shear for the test-braced frame was also $0.2W = 70.7$ kN, which resulted in the target SCED design forces shown in Table II. Due to limited availability of structural shapes and tendons, only the first story SCED initial stiffness requirements could be exactly satisfied in the test frame. Other brace stiffness properties exceeded the required values, which led to a relatively stiffer test frame compared with the prototype frame.

The test frame columns were HSS152 × 76 × 8.0 oriented in the weak axis. This column design was adopted to simulate the approximate combined flexural stiffness of a quarter of all of the building's columns in the direction of the frame, including the braced frame columns in the strong direction, the moment frame columns in the weak direction, and the gravity columns. Hence, the beneficial stiffening effect of continuous columns over the height of the building could be included in the test. The beams were selected during the test frame design.

Table I. Prototype SCED frame properties.

Story	kN Story shear V_{xi}	kN Target SCED force P_T	kN/mm Initial stiffness k_1	Post-activation stiffness ratio r	kN SCED activation force P_a	kN SCED external fuse activation P_u
3	309	379	128	0.024	373	589
2	527	646	188	0.028	654	1011
1	637	780	235	0.026	841	1269

Table II. Test SCED frame properties.

Story	kN Story shear V_{xi}	kN Target SCED force P_T	kN/mm Initial stiffness k_1	Post-activation stiffness ratio r	kN SCED activation force P_a	kN SCED External fuse activation P_u
3	35.4	44	78.8	0.043	44	123
2	58.7	72	78.8	0.043	72	150
1	70.7	87	78.8	0.043	87	164

3. TEST FRAME DESIGN AND SETUP

The shake table test setup is shown in Figure 3. The multi-story SCED-braced frame was attached to the shake table via pin connections at the bases of the columns. The HSS beams and connections were designed to have a high axial stiffness and a low rotational stiffness at the ends. This simulates a shear tab connection, which will typically allow for some rotation at the ends of the beams in a braced frame. The lateral support for the braced frame was provided by a steel lateral support frame that surrounds the shake table (not shown in the figure for clarity). The lateral restraint supports shown in Figure 3 served as an interface between the larger lateral support frame and the test frame, ensuring that the test frame did not move out of plane.

The required seismic mass could not be accommodated on the shaking table due to payload limitations. Therefore, a mass simulation frame was erected in series with the test frame. This mass simulation frame consisted of steel plates that simulate the horizontal mass and gravity load of one-quarter of the scaled-down prototype building [25]. These plates were supported between the stories by columns with friction-free rockers at their upper and lower ends. At the base of the mass simulation frame, the columns were mounted on a horizontal steel frame that sat on low friction roller bearings. That base frame was horizontally connected to steel members that were attached to the shake table surface. Using this arrangement, the mass simulation frame was able to impose consistent P-Delta lateral forces to the test frame. The mass simulation frame was connected to the test frame at every story using stiff HSS beams, which were installed in series with a load cell to directly measure the applied horizontal inertia

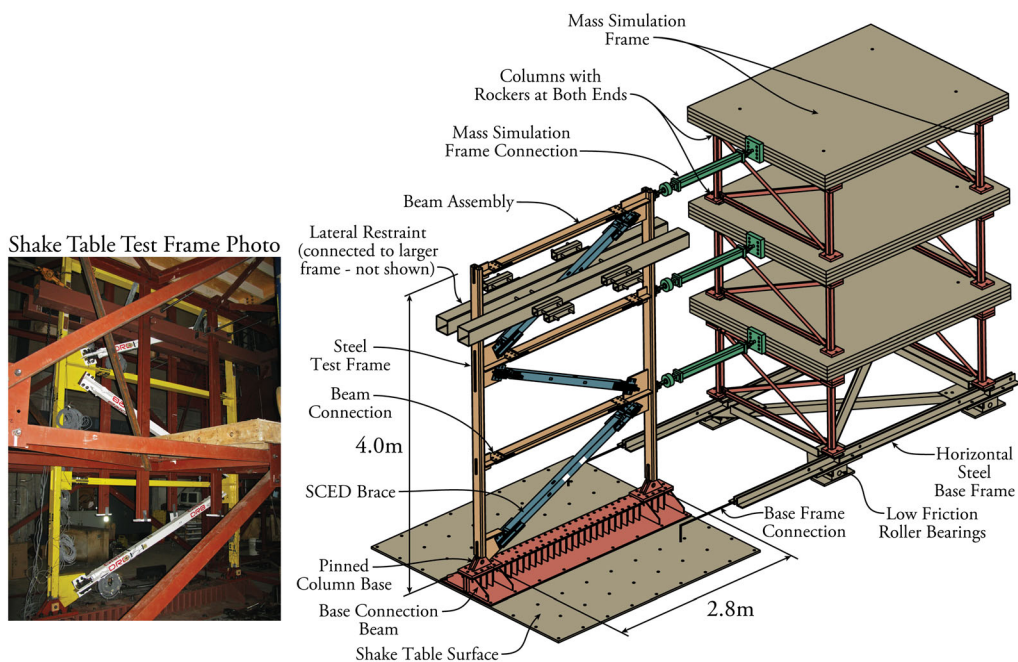


Figure 3. Test frame and mass simulator.

forces and, thereby, obtain story shears. Strain gages on the columns and braces measured axial, shear, and moment in those members. String potentiometers were used to measure the lateral deflections of each story and of the table itself and the axial elongation of the braces. Accelerometers on the table, the frame at each level, and the mass at each level measured lateral accelerations. Due to the high stiffness of the SCED-braced frame test structure, it was not possible to characterize vibration periods and damping coefficients accurately for the specimen.

4. MODELING OF THE TEST STRUCTURE

4.1. OPENSEES model

The full test structure was modeled in 2D using the nonlinear dynamic modeling software OPENSEES [26]. At that time, no model in OPENSEES existed that could adequately model the behavior of a self-centering brace; therefore, a custom material model was developed for this purpose. This material model, the ‘Self-Centering’ uniaxial material, is now included in the main OPENSEES distribution. It accepts parameters for the initial stiffness, activation load, post-activation stiffness ratio, and hysteresis width parameter, and also allows for the modeling of external fuse slip and lock up of the brace mechanism. Details regarding the function and use of this model may be found in the OPENSEES online manual [27].

To analyze the response of the test frame after the tests were complete, we constructed an OPENSEES model as shown in Figure 4. The shake table was modeled as a rigid foundation. The actual acceleration that was recorded at the base of the test specimen on the shake table was applied at the bottom of the structure.

The modeled hysteresis of a SCED brace is shown on the right side of Figure 4. The key parameters are the initial stiffness k_1 , the activation load P_a , the post-activation stiffness k_2 , the post-activation stiffness ratio r (redundant with k_2), and the hysteresis width parameter β . The external friction fuse activates when the brace mechanism reaches a predicted maximum elongation (at axial load P_u). It limits the axial force in the brace and allows for increased elongation capacity of the bracing system.

4.2. OPENSEES model assumptions and simplifications

The mass of the frame and mass simulation system were lumped at the closest nodes. The mass simulation system itself was modeled as a single multi-story leaning column consisting of three vertical truss elements with mass and weight of the real mass–simulation system being assigned at each level. This system was connected to the main frame in the model by truss elements with stiffness equivalent to the actual HSS beams that connect the mass simulation system to the test frame (no diaphragm constraints were used).

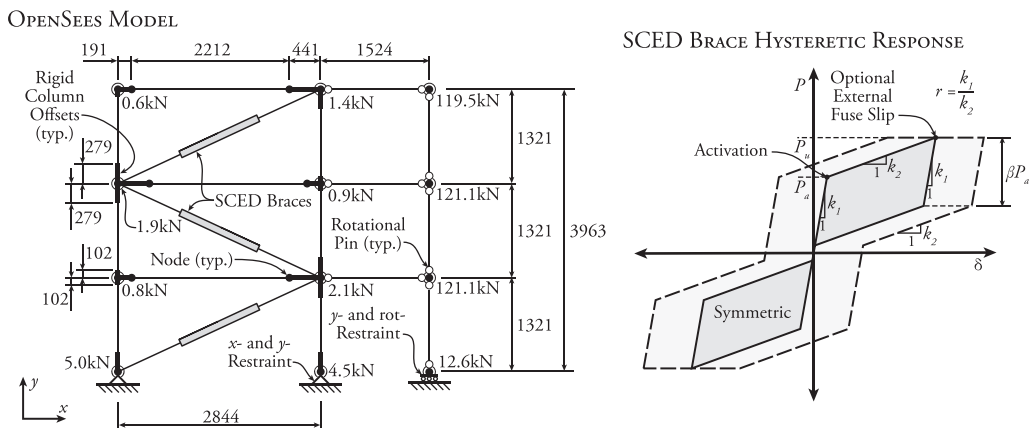


Figure 4. OPENSEES model of the test frame and self-centering energy dissipative (SCED) brace element hysteresis.

Vertical rigid end offsets were assigned to the test frame columns to simulate the physical dimensions of the gusset plates in the corners. The beams were modeled using three elements in series. The left and right elements are stiff beam members with full-length rigid offsets representing the gusset plates. The center element represents the beam member itself with fiber-section lumped plasticity hinges at either end to model the behavior of the flexible horizontal splice plate end connections.

Inherent damping was modeled using Rayleigh damping in modes 1 and 3. Different amounts of damping were tested to check the sensitivity of the model, which will be described further in Section 7.

4.3. SAP2000 model

In addition to the primary OPENSEES model of the structure that was used for prediction and evaluation of the response of the structure, a parallel simplified model was built using the commercial structural analysis software package SAP2000 [28]. The purpose of this model was to compare the more sophisticated OPENSEES model with one that is more likely to be used in a design setting. The method that was used to simulate SCED braces in SAP2000 has been previously described in the works of Le Bec *et al.* [29] and Erochko [30]. This model had the same dimensions, linear frame properties, rigid end offsets, and mass as the OPENSEES model; however, the simplified SAP2000 model used pinned ends for the beams because practicing engineers are unlikely to model all beam–column joints using plastic hinges. The nonlinear time history analysis was performed using the Ritz vector analysis method because this was found to be orders of magnitude faster than the full direct integration method for this type of structure. The drawback of using the Ritz vector method in SAP2000 was that P-Delta effects could not be considered in the analysis. It was also not possible to create a stable model in SAP2000 that included the response of the external friction fuse in series with the brace. Constant inherent damping of 1% of critical was provided in all modes.

5. SCED BRACE DESIGNS AND PRELIMINARY QUASI-STATIC BRACE TESTS

The same SCED brace design was used to achieve the design targets for all three stories (Table II). The brace design is detailed in the work of Kim [19], and a schematic of the brace specimen is shown in Figure 5. The SCED braces that were designed and fabricated for the test frame utilized a single tendon and a friction damper as the energy dissipation device. The outer member of each brace was an HSS100 × 100 × 4.0 steel tube, and the inner member was an HSS75 × 75 × 4.5 steel tube. DRB Inc. (Seoul, Korea) used tendons made of a straight fiber a straight fiber, 17-mm nominal diameter Technora aramid rope with aluminum spike and barrel anchors. The friction damper interfaces consisted of stainless steel on one side and non-asbestos organic friction pads on the other. The normal force for the friction interfaces was provided by 0.5 in steel bolts. An external friction fuse was included for each brace, which used a similar stainless on non-asbestos organic friction pad interface and larger 0.75 in steel bolts. The varying activation forces for each story of the test frame in Table II were achieved by using different tendon pretension forces and friction interface normal forces.

Before they were installed in the frame, each brace was individually tested axially in a load frame. Figure 6 shows the resulting hysteretic response of each brace. Initially, the bolts that provide the normal force for the internal friction dampers were loosened (giving results shown in Figure 6 as ‘Tendon-Only’). When the braces were tested in this condition, the ideal hysteresis was expected to be bilinear elastic (with an initial and post-activation stiffness but with little energy dissipation). The experimental tendon-only hystereses shown in Figure 6 exhibited a non-zero width, which indicated that energy was being dissipated through inherent friction present in the mechanism, including a portion that came from the un-tightened dampers. It is clear from these hystereses that the SCED braces were functioning as intended and experienced a full self-centering behavior. The width of the curve at zero axial force is due to the friction in the system that acts during the linear deformation range (pre-activation). This width seems exaggerated in these plots because the total deformation in these tests was limited to 4 mm (only 15% of the total self-centering elongation capacity of 27 mm) to avoid any significant loading of the SCED braces prior to the shake table tests.

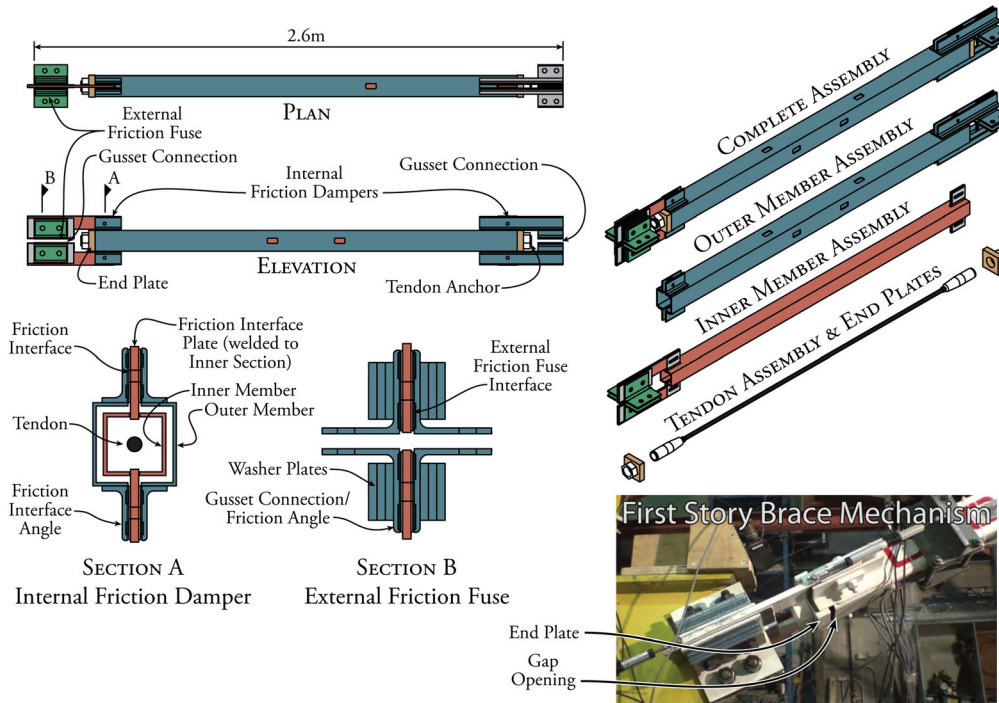


Figure 5. self-centering energy dissipative brace schematic.

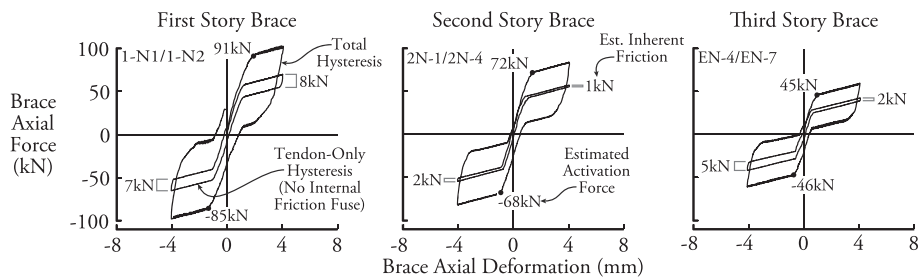


Figure 6. Brace only test results.

6. SELECTION OF GROUND MOTIONS

Four groups of ground motions were used for the shake table tests, with each group representing a different phase of the testing program. The selected records with their properties and applied scaling factors are shown in Table III. All of the records are also scaled in time by a factor of 0.577 as described in Section 2. The selection of the records for each phase is described later in the text.

Phase 1 consisted of three different records for Los Angeles taken from the suite of records of the SAC joint venture project [31] for a probability of exceedence of 50% in 50 years. Phase 2A consisted of two records for Los Angeles that have a probability of exceedance of 10% in 50 years. These records were from the online PEER NGA database and scaled as per the instructions in FEMA P695 specification [32] and then further scaled to achieve a maximum drift of approximately 2% in the first story SCED brace. Phase 2B consisted of a single high acceleration record to simulate an event with a probability of exceedance of 2% in 50 years. Phase 3 consisted of a subduction type earthquake record. For this single test, the historical 2003 Tokachi-Oki subduction record was used and scaled up to match the 10% in 50-year spectrum for Los Angeles. Records for phase 4 of the project were selected to represent the

Table III. Earthquake record properties and scaling

No.	Record	Year	Name	Station	M	R (km)	SAC/ATC scale fact.	DBE/MCE scale fact.	%EQ	Total scale fact.
1-1	SAC LA50	1984	Morgan Hill	gil3	6.2	15	2.35	1.00	30	0.71
1-2	SAC LA50	1984	Morgan Hill	gil3	6.2	15	2.35	1.00	50	1.18
1-3	SAC LA50	1984	Morgan Hill	gil3	6.2	15	2.35	1.00	100	2.35
1-4	SAC LA53	1966	Parkfield	cs08	6.1	8.0	2.92	1.00	100	2.92
1-5	SAC LA55	1986	N Palm Springs	plma	6.0	9.6	2.75	1.00	100	2.75
2-1	ATC N09B	1994	Northridge	Rinaldi	6.7	10.9	0.69	1.33	50	0.46
2-3	ATC N01B	1979	Imperial Valley	El C. 6	6.5	27.5	0.9	1.33	90	1.08
2-4	KOBE 01B	1995	Kobe	Takatori	6.9	13.1	1.00	1.00	90	0.90
3-1	SUBMod-F01B	2003	Tokachi-Oki	84km Station	8.0	84	1.00	1.00	300	3.00
4-1	SAC LA-50	1984	Morgan Hill	gil3	6.2	15	2.35	1.00	100	2.35
4-2	MTL 02	SIM	Sim. Montreal No. 2	N/A	7.0	42	1.00	1.00	250	2.50
4-3	CVX31	SIM	Sim. Charlevix No. 31	N/A	7.0	26	1.00	1.00	110	1.10

demands of eastern North American earthquakes. Two of these were simulated records created by Atkinson [33]. To compensate for the difference between the seismic demand for eastern North America and the seismic demand for Los Angeles that the test frame was designed for, these phase 4 records were scaled up by a ratio of the design spectrum value for Los Angeles to the design spectrum value for each site at the design period.

7. SHAKE TABLE TEST RESULTS AND DISCUSSION

A summary of the maximum response for all of the shake table tests is shown in Table IV. This table summarizes the experimental results, the corresponding OPENSEES model results, and selected SAP2000 model results. Inherent damping in the models was modeled by providing 1% of critical damping. Rayleigh damping was used for the OPENSEES model, and constant damping was used for the SAP2000 model. Values between 1% and 3% were tested in the models, but 1% was selected because it gave the best match for the story drift and shear values for the moderate to high acceleration earthquakes.

Sample time history drift and hysteretic responses from tests are shown in Figure 7. The results demonstrate the diversity of the shake table excitations that were chosen and the consistent response of the SCED braces that were obtained for all of these records. One sample record is shown from each phase of the testing program. Peak drift values for these records may be found in Table IV. Only test results are shown in Figure 7 in the interest of clarity; individual test/model comparisons will follow. Test 1-4A represents a 50% in 50-year hazard level excitation with a moderate duration. In this record, the SCED braces at all three stories activate. The first story in particular experiences approximately ten cycles of activation. Test 2-1A represents a 10% in 50-year hazard level excitation with higher maximum drift and a balanced response in both directions. Under this record, the braces experience more drift than in test 1-4A; however, the response is characterized by a couple of large cycles rather than a large number of smaller cycles. Test 2-4A represents a 2% in 50-year hazard level excitation with high drifts, external fuse activation in the first story in both directions, and good propagation of the drift demand into the second and third story braces above. The hysteretic response of the first brace shows that the external fuse activated in both directions, resulting in a small residual drift of <0.5%. The behavior of the test frame subjected to this record will be discussed in further detail in a following section. Test 3-1A represents a long duration subduction-type earthquake. As these plots show, when subjected to this long earthquake, the first story brace undergoes approximately 20 cycles of activation. Even though the brace activates so many times, the shape of the hysteretic response remains consistent and shows no significant degradation. Moreover, the SCED brace experiences no residual drift during consecutive activation cycles and at the end of the excitation. Finally, test 4-3A represents a simulated East Coast

Table IV. Experimental results versus model results. Experimental result (OPENSEES result with 1% damping) [SAP2000 result with 1% damping].

EQ	PGA (g)	Acceleration (g)			Story shear (kN)	
		S1	S2	S3	S1	S2
1-1	0.16	0.19 (0.32) [0.31]	0.15 (0.30) [0.28]	0.15 (0.37) [0.37]	39 (66) [67]	35 (58) [59]
1-2	0.27	0.28 (0.41) [0.39]	0.22 (0.48) [0.44]	0.25 (0.41) [0.41]	66 (68) [69]	50 (66) [67]
1-3	0.59	0.50 (0.50) [0.56]	0.38 (0.68) [0.70]	0.41 (0.44) [0.44]	92 (86) [85]	70 (71) [70]
1-4	0.69	0.51 (0.84) [0.86]	0.41 (0.94) [0.96]	0.42 (0.48) [0.50]	95 (104) [101]	72 (76) [76]
1-5	0.52	0.50 (0.71) [0.72]	0.62 (0.75) [0.76]	0.95 (0.61) [0.61]	129 (114) [111]	100 (89) [98]
2-1	0.22	0.47 (0.83) [0.81]	0.38 (0.60) [0.54]	0.43 (0.48) [0.45]	102 (95) [93]	79 (87) [87]
2-3	0.35	0.48 (0.73) [0.71]	0.46 (0.48) [0.54]	0.45 (0.44) [0.44]	138 (128) [126]	91 (93) [89]
2-4	0.54	0.87 (1.07)	0.71 (1.04)	0.87 (1.02)	192 (179)	139 (157)
3-1	0.28	0.39 (0.76) [0.76]	0.40 (0.53) [0.52]	0.43 (0.41) [0.40]	108 (109) [107]	86 (82) [84]
4-1	0.55	0.60 (0.59)	0.38 (0.58)	0.39 (0.41)	92 (88)	72 (65)
4-2	0.51	0.50 (0.58)	0.32 (0.44)	0.32 (0.40)	73 (78)	58 (60)
4-3	0.36	0.42 (0.60)	0.34 (0.40)	0.37 (0.40)	79 (75)	60 (60)

earthquake response characterized by higher frequency ground accelerations with higher drifts in the one direction than the other. Again, the self-centering capability of the SCED braces prevents this acceleration that is strongly biased in one direction from causing residual drift in the frame.

As can be seen in Table IV, the OPENSEES and SAP2000 models, despite their differing levels of sophistication, result in similar good quality predictions for the behavior of all the SCED braces in the multi-story frame. Figure 8 shows a comparison of some of the detailed results of these two different models for two selected test earthquakes. As this figure shows, the two models provide almost identical predictions for the hysteretic response. In addition, both models provide an accurate representation of the response of the test frame, suggesting that the simplified SAP2000 model would be useful to practicing engineers for designing SCED-braced frames. A more comprehensive comparison of the two models results with respect to the shake table test results is shown in Figure 9. In this figure, the maximum values of floor acceleration, story shear, story drift, and column axial force are given for each test model relative to the recorded response of the shake table test structure. Each test model (either OPENSEES or SAP2000) is plotted at a location on the x -axis corresponding to the maximum drift that was recorded for that test in the real structure. This figure shows that the story shear, story drift, and column axial loads are all well predicted by the model except at the lowest maximum drift amplitudes and that the OPENSEES and SAP2000 models provide similar predictions for each test. The peak accelerations that are predicted by the models, however, are generally greater than those that were experienced in the tests. The reason for this discrepancy will be discussed in detail in a later section.

7.1. Hysteretic response, drift results, and comparison with model predictions

The shake table tests demonstrated that the hysteretic response of the SCED braces was both stable and repeatable under a large number of cycles of deformation (over more than 12 strong ground motions). Using the measured hystereses, the total activation force for each brace was determined after each test, and these results showed that there was no appreciable drop in activation force as a result of internal friction fuse degradation. Some sample drift responses and hysteretic plots for individual shake table tests are shown with their corresponding model results in Figure 10.

The first results shown in Figure 10 are for the first story of the test frame subjected to the long duration Tokachi-Oki subduction earthquake (test 3-1A). This type of earthquake has the potential to result in progressive collapse for traditional hysteretic yielding or friction systems. The SCED braces, however, did not experience any significant residual drift. The drift plot shows that the drift histories and peak drift values are similar between the experiment and the OPENSEES and SAP2000 models. The accompanying hysteresis plot on the right shows that the real SCED brace was able to resist dozens of activation cycles without any change in its response. The experimental hysteretic response is also well matched by the prediction of the analytical model.

Story shear (kN)	Drift (%)				Column Axial (kN)	
	S3	S1	S2	S3	L	R
16 (44) [44]	0.08 (0.13) [0.14]	0.05 (0.09) [0.12]	0.05 (0.08) [0.10]	0.05 (0.08) [0.10]	22 (47) [44]	38 (73) [79]
30 (49) [48]	0.16 (0.19) [0.19]	0.11 (0.19) [0.21]	0.09 (0.15) [0.16]	0.09 (0.15) [0.16]	33 (51) [52]	60 (84) [86]
44 (52) [53]	0.61 (0.51) [0.48]	0.30 (0.28) [0.29]	0.17 (0.22) [0.25]	0.17 (0.22) [0.25]	48 (55) [57]	85 (91) [92]
48 (52) [60]	0.67 (0.83) [0.80]	0.35 (0.45) [0.45]	0.20 (0.36) [0.36]	0.20 (0.36) [0.36]	48 (61) [63]	89 (103) [102]
71 (72) [73]	1.31 (1.09) [1.07]	0.87 (0.67) [0.71]	0.63 (0.61) [0.59]	0.63 (0.61) [0.59]	66 (67) [68]	116 (118) [118]
46 (57) [54]	0.87 (0.70) [0.69]	0.46 (0.46) [0.49]	0.29 (0.39) [0.37]	0.29 (0.39) [0.37]	56 (57) [60]	91 (98) [100]
50 (52) [52]	1.60 (1.25) [1.23]	0.82 (0.77) [0.76]	0.27 (0.31) [0.32]	0.27 (0.31) [0.32]	68 (68) [67]	119 (115) [111]
97 (122)	3.96 (3.26)	2.00 (1.99)	1.39 (1.63)	1.39 (1.63)	102 (115)	171 (194)
45 (48) [48]	1.00 (0.91) [0.89]	0.64 (0.59) [0.61]	0.21 (0.25) [0.25]	0.21 (0.25) [0.25]	52 (59) [61]	99 (113) [113]
46 (48)	1.09 (0.93)	0.59 (0.41)	0.21 (0.20)	0.21 (0.20)	77 (55)	87 (85)
39 (45)	0.74 (0.71)	0.15 (0.27)	0.12 (0.15)	0.12 (0.15)	66 (50)	75 (75)
38 (46)	0.87 (0.67)	0.28 (0.28)	0.11 (0.11)	0.11 (0.11)	59 (49)	75 (78)

SHAKE TABLE TESTS: SAMPLE DRIFT AND HYSTERETIC RESPONSES

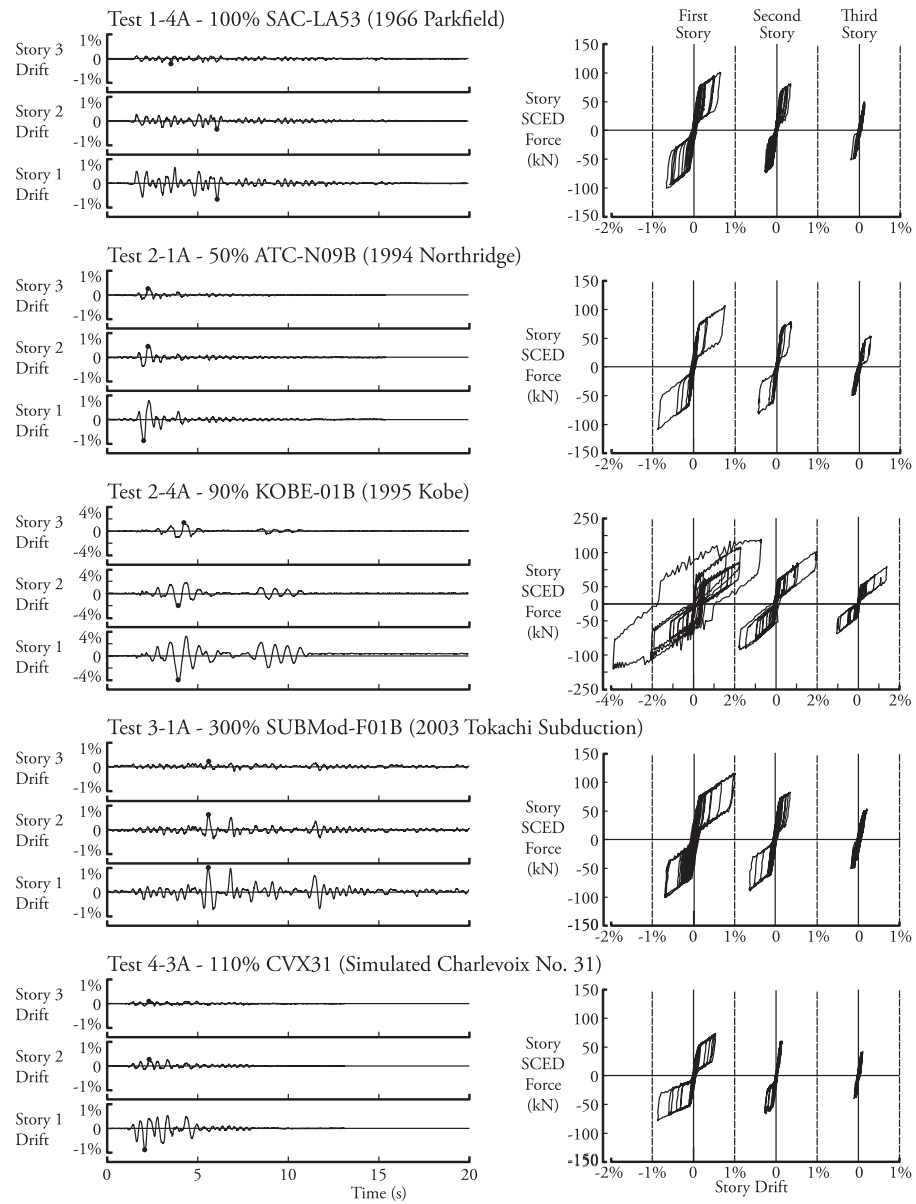


Figure 7. Sample shake table test results—drift time histories and brace hysteresees.

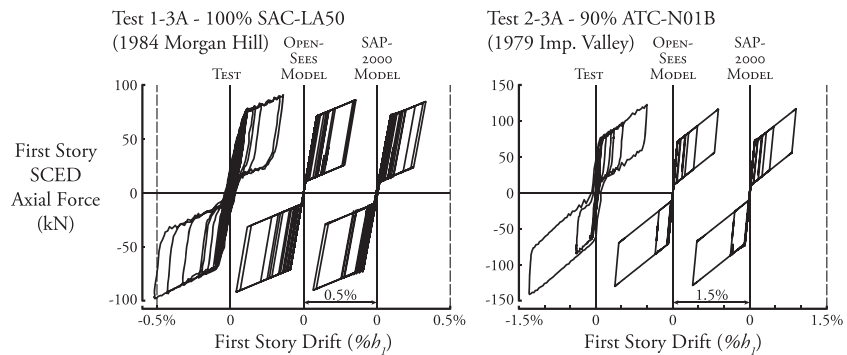


Figure 8. Comparison of SAP2000 and OPENSEES model results.

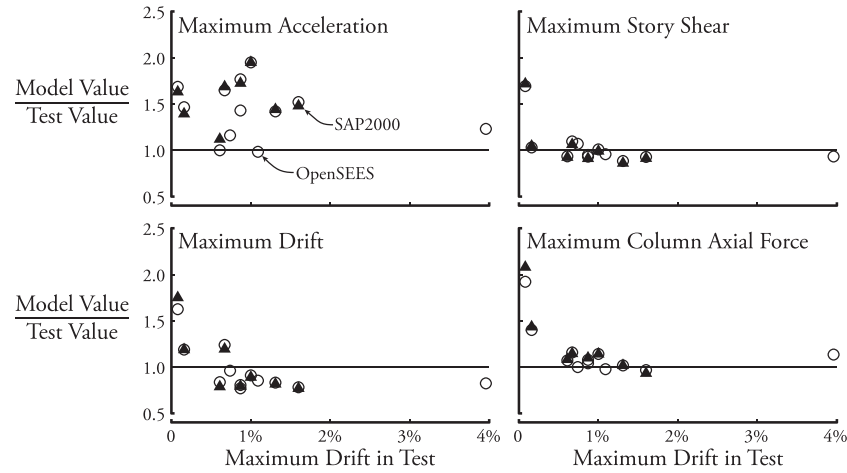


Figure 9. Comparison of test results with both computer models.

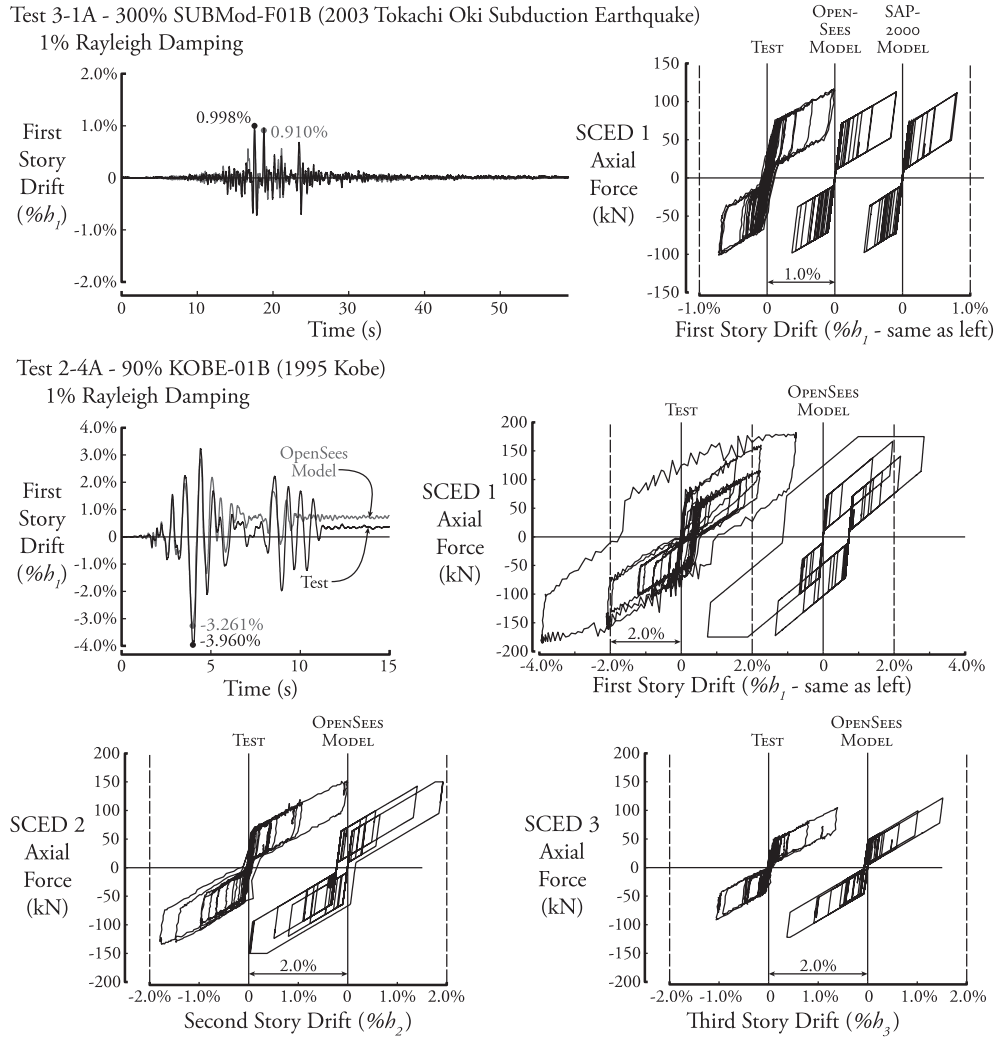


Figure 10. Sample drift and hysteretic responses (experiment vs. model).

The second set of results in Figure 10 shows the response of the frame subjected to the largest amplitude record that was used—the 1995 Kobe earthquake. The time history of the drift response for the first story is shown along with the hysteretic response of the SCED braces at all three stories. Under this record, the first story experienced drifts on the order of 4.0%, which activated the external friction fuse. This activation is indicated by the horizontal (zero stiffness) sections of the first story hysteresis. Because it was not possible to model the external friction fuse in SAP2000, only the OPENSEES model results are shown for this record. As the plots show, the first story brace experienced considerable external fuse movement in both directions, producing a residual drift of approximately 0.3% in the experimental results and approximately 0.7% in the OPENSEES model results as shown in the drift time history on the left side. The model predicts the hysteretic response very well, and the lower two hysteresis plots show that the model also predicted the response of the second and third story braces well.

During this excitation, the first story brace experienced a slight drop in activation force after the peak cycle. This likely occurred because the tendon in the brace was not pre-elongated enough during the manufacturing process and does not reflect any poor behavior on the part of the friction damper. The initial loading stiffness of the aramid tendons is less than the stiffness of the tendon under subsequent cycles; therefore, the tendon must be pre-elongated to the maximum expected load prior to locking it off at the target rest pretension. Hyper-elongation of the tendon of only a few millimeters past the pre-elongation strain resulted in this drop in the tendon pretension load. This experience emphasizes the need for a well-enforced tendon tensioning method; however, the drop in activation force did not negatively affect the ability of the brace to resist the considerable deformation demand imposed on it by the Kobe record.

Because the residual drift that remained in the first story SCED brace after test 2-4 was not much larger than the AISC erection tolerance for columns of 1/500 [34], the frame was not adjusted, and later tests were conducted using the new position as the reference point for zero drift.

7.2. Acceleration results and comparison to model predictions

One of the goals of this shake table study was to assess the acceleration response of multi-story SCED-braced frames and to determine whether the high peak accelerations that were observed in previous numerical studies [18, 24] were caused by a real phenomenon or were entirely or partially numerical.

Self-centering systems are unique in that they experience a low to high stiffness transition at high velocity as they pass through zero deformation. Typically, when a self-centering system returns towards zero deformation, it does so at a relatively low stiffness. Near zero deformation, the initial high stiffness of the system is recovered before it can activate in the opposite direction. Because the system has momentum as it passes through zero, this transition tends to occur at high velocity, in contrast to when the system is changing directions at peak deformation when the velocity tends to be lower.

Because the stiffness changes in a SCED-braced frame tend to occur at high velocity, the forces in the braces also change quickly, easily causing large imbalances between the forces in braces in adjacent stories if they do not change stiffness at the exact same time. This imbalance in the SCED forces above and below a given story causes the presence of a floor acceleration, which is required to satisfy dynamic horizontal equilibrium (Figure 11). In the figure, the force caused by that floor acceleration, $F_{inertia}$, is shown. Shears in the columns and the damping force are typically small

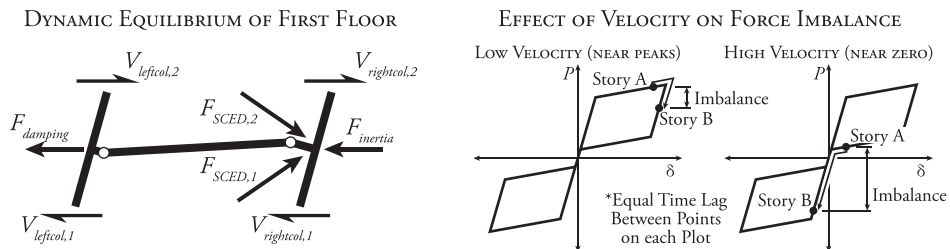


Figure 11. First floor dynamic equilibrium and effect of velocity on force imbalance.

compared with brace forces in braced frames, and therefore the accelerations are mostly caused by the brace force difference. Figure 11 also shows the reason why high velocity stiffness transitions tend to produce larger force differences and, therefore, higher peak accelerations in self-centering systems. This simplified figure assumes that SCED braces of two adjacent stories have a similar hysteretic shape. If it is assumed that the time lag between the responses of the braces in two adjacent stories is approximately constant, then less distance will be traveled around the hysteresis in that amount of time when the velocity is low than when it is high. Accordingly, the distance between the two SCEDs on the hysteresis will also be higher when the velocity is high. Larger distances mean larger force imbalances when the stiffness changes, which in turn result in higher peak floor accelerations. Inertial floor accelerations caused by the braces are however limited by the maximum difference between the forces in the two SCED braces, equal to the sum of the highest axial load that is possible for each brace.

The effect of low to high stiffness transitions at high velocities was observed and quantified by Wiebe and Christopoulos [35] using a two degree of freedom numerical model, but it has never been studied or observed experimentally. An additional study by the same authors [36] found that introducing rounded corners to provide a gradual stiffness transition to the hysteretic response of the nonlinear element mitigates the acceleration spikes in the same two degree of freedom system model.

As shown in Table IV, the absolute peak story accelerations that were recorded during testing were generally well-controlled and in the range of approximately 0.5 g for all but the largest earthquake records (with the notable exceptions of records 1-5 and 4-1, which are actually the same record for comparison, and the 2% in 50-year record number 2-4). Even those largest records showed peak accelerations under 1.0 g in the worst cases. However, as shown in Figure 9, the OPENSEES and SAP2000 models tended to significantly overestimate the magnitude of these peak floor accelerations in most cases.

The acceleration responses of the test frame and the model were compared and investigated in detail to determine the cause of this overestimation. Figure 12 shows a comparison of the test versus model accelerations for the first floor of the frame subjected to 50% of the Northridge earthquake. Because the OPENSEES and SAP2000 model results were similar, only the OPENSEES results are shown here for

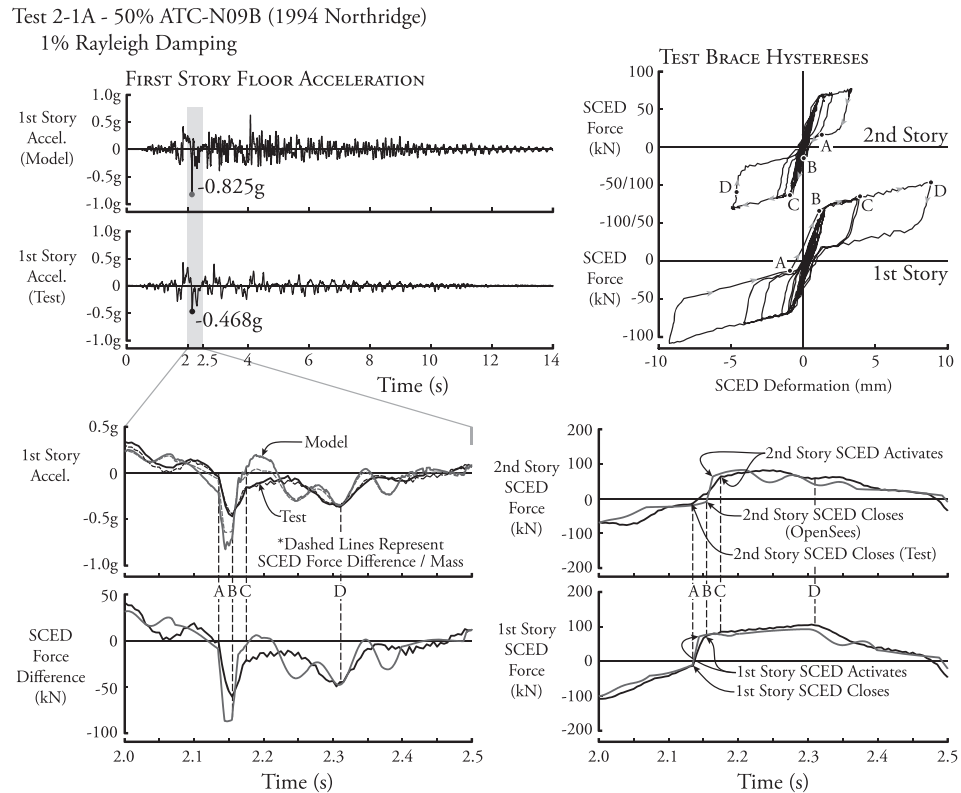


Figure 12. Sample acceleration spike response.

clarity. In general, the time traces of the accelerations have a similar shape, except that the model response has a series of spikes superimposed on the underlying acceleration pattern. To show the cause of these acceleration spikes, the first floor acceleration response with the forces that are present in the SCED braces above and below the first floor level were compared. The hysteretic responses of those SCED braces are also shown at the top right of the figure.

Before the acceleration spike is present (prior to time A in the figure), the SCED braces both above and below the first story are returning towards zero brace deformation at low stiffness (stiffness k_2). At time A, the first story SCED mechanism closes (in both the test and the model), causing the stiffness of the brace to revert to the higher initial stiffness k_1 . This causes the first story brace to accumulate force quickly; however, due to the inertia of the mass of the first floor, there is a time lag between the closure of the first and second story brace mechanisms. The second story brace is not able to close until time B at which point the first story brace has already activated. Between time A and time B, the force in the second story brace does not accumulate as quickly as the force in the first story brace. This sudden, short duration force imbalance results in a high acceleration between time A and time B that works to counteract the force imbalance and maintain the floor equilibrium. The difference between the axial force in the first and second story SCED braces is shown in the plot at the bottom left. When this force is projected into the horizontal direction and divided by the floor mass, the resulting calculated acceleration is almost identical to the measured acceleration as shown by the dashed lines in the first story acceleration plot. This shows that the acceleration in the real frame is mostly caused by this SCED force imbalance as suggested previously. For the OPENSEES model results, the measured and calculated accelerations are close but do not exactly match up at the peaks. This difference between the two values is caused by shear forces in the columns resulting from the lateral behavior of the frame. At that particular time in the test, there was less shear force in the test columns than there was in the model columns.

At time D, the first story brace reverses direction and changes stiffness again. This change represents the type of low velocity stiffness transition that hysteretic-type systems generally experience. As the first story SCED force plot shows, even though the brace stiffness after the change at time D is the same as it was after the stiffness change at time A, the force in the brace changes much more slowly because the velocity at time D is lower. Accordingly, the force imbalance at time D is lower, as is the acceleration in both the test and the model.

The peak acceleration is much lower in the test than in the model because the test braces provide smoother transitions in time between the low and high stiffness. This gradual transition reduces the difference between the forces in the SCEDs above and below the first floor, thereby reducing the necessary counteracting acceleration. Therefore, although the shake table tests have proved that the peak accelerations caused by high velocity stiffness transitions exist and are significant, in practice, real self-centering systems have a somewhat gradual stiffness transition, which mitigates the severity of these accelerations. The consequence of this is that models of self-centering systems that use sharp stiffness transitions will tend to significantly overestimate peak accelerations. To get a better estimate of the peak accelerations, a more realistic gradual transition could be modeled using the method described in the work of Wiebe and Christopoulos [36]. These results also suggest that, although high magnitude acceleration spikes can exist in self-centering systems by explicitly designing these systems to change stiffness gradually, these peak accelerations may be significantly reduced.

7.3. Story shear results and the effect of inherent damping

Similar to the story drift results, the experimental story shear results in Table IV are in good agreement with the predictions of the models. As mentioned previously, the inherent damping value of 1% of critical was selected on the basis of the quality of the prediction that the models achieve with regards to the story drifts and shears. These inherent damping models, all of the sources of damping that are not explicitly provided to the system by the SCED braces; these sources include friction inside frame component connections, friction between the test frame and the lateral support. However, this value of 1% for inherent damping does not seem to be appropriate for all excitation amplitudes.

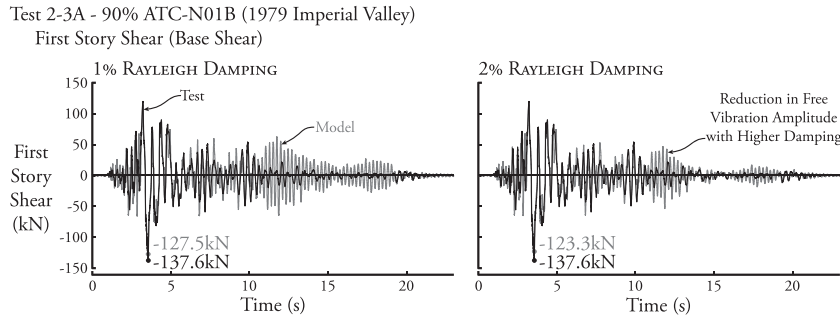


Figure 13. Reduction of free vibration base shear amplitude with added inherent damping.

Towards the end of the time history in some of the models, when the model is responding predominantly in a damped free vibration mode, this low inherent damping value causes the story shear to take an unrealistically long time to damp out. Figure 13 shows the base shear response of the test frame subjected to the 1979 Imperial Valley earthquake. Again, only the OPENSEES model results are shown here for clarity. The left side of the figure shows the response of the experiment compared with the response of the model using 1% inherent damping, and the right side shows the same experimental data and the model using 2% inherent damping instead. The experimental data show that the free vibration response at the end of the record quickly damps out in reality. The model under 1%, however, exhibits a significant vibration that is not observed in the experimental results. Increasing the inherent damping to 2% reduces this effect, but also reduces the peak story shear.

What seems to be necessary here is the ability to model low inherent damping for large cycles and significantly higher inherent damping for the small cycles of response. The discrepancy between the two levels of response with respect to inherent damping is likely occurring because the inherent damping in the shake table frame is predominantly caused by friction. However, the inherent damping is modeled using the Rayleigh damping model, which is proportional to the velocity. Friction causes a relatively greater amount of inherent damping in the low magnitude cycles, when the velocity is low, than in the high cycles when the velocity is high.

8. CONCLUSIONS

The shake table tests that were conducted on a multi-story SCED-braced frame successfully demonstrated that the SCED bracing system performed as designed when subject to a fully dynamic base excitation and that the companion OPENSEES computer model was capable of predicting the results of the tests. The SAP2000 model was able to predict the results equally well, with the limitation that it could not model the external friction fuse behavior.

The braces were able to withstand 12 consecutive earthquakes without damage or loss of friction fuse capacity. In addition, the external friction fuses that are in series with the braces worked as expected, extending the drift capacity of the braces from 2% to 4% of story height.

The peak drift results, peak story shear results, and peak column axial loads were well-predicted by both the OPENSEES and the simplified SAP2000 numerical models of the structure.

The peak story accelerations in SCED-braced frames are due to high velocity brace stiffness transitions causing force imbalances between the SCED braces in adjacent stories. The peak story accelerations were generally overestimated in the models due to the sharp transitions in the brace forces predicted by the SCED brace model; more gradual stiffness transitions in the model would likely result in more accurate predictions of peak floor accelerations.

On the basis of the results of these tests, self-centering energy dissipative (SCED) braces may be considered an effective stand-alone lateral force resisting system for multi-story steel frames. They provide a high performance, fully self-centering response under design-level seismic hazards with a probability of exceedance of 10% in 50 years and an increased performance level with reduced residual drifts when subjected to maximum-credible-level events with a probability of exceedance of 2% in

50 years. Additionally, design engineers may feel confident that numerical models of SCED-braced systems that utilize either the ‘Self-Centering’ uniaxial material in OPENSEES or the simulated SCED model in SAP2000 will be robust and will provide meaningful predictions of the overall seismic response of buildings incorporating SCED braces.

ACKNOWLEDGEMENTS

Financial assistance for the research project described in this paper was provided by the Natural Sciences and Engineering Research Council of Canada (NSERC) through the Idea to Innovation Program. Dungil Rubber Belt Co., from Busan, Korea, provided funding and supplied the SCED brace specimens for the shake table test program.

The authors would also like to acknowledge the assistance provided by the staff of the structural engineering laboratory at École Polytechnique of Montreal.

REFERENCES

- Pampinan S, Christopoulos C, Priestley MJN. Performance-based seismic response of frame structures including residual deformations. Part II: multi-degree of freedom systems. *Journal of Earthquake Engineering* 2003; **7**(1):119–147. DOI: 10.1080/13632460309350444
- Ruiz-García J, Miranda E. Residual displacement ratios for assessment of existing structures. *Earthquake Engineering and Structural Dynamics* 2006; **35**(3):315–336. DOI: 10.1002/eqe.523
- Erochko J, Christopoulos C, Tremblay R. Residual drift response of SMRFs and BRB frames in steel buildings designed according to ASCE 7-05. *Journal of Structural Engineering* 2011; **137**(5):589–599. DOI: 10.1061/(ASCE)ST.1943-541X.0000296
- McCormick J, Aburano H, Ikenaga M, Nakashima M. Permissible residual deformation levels for building structures considering both safety and human elements. *Proceedings of the 14th World Conference on Earthquake Engineering*, Beijing, China, 2008; Paper No. 05-06-0071.
- MacRae GA, Kawashima K. Post-earthquake residual displacements of bilinear oscillators. *Earthquake Engineering and Structural Dynamics* 1997; **26**(7):701–716. DOI: 10.1002/(SICI)1096-9845(199707)26:7<701::AID-EQE671>3.0.CO;2-I
- Priestley MJN, Sritharan S, Conley J, Pampinan S. Preliminary results and conclusions from the PRESSS five-story precast concrete test building. *PCI Journal* 1999; **44**(6):42–67.
- Christopoulos C, Filiatrault A, Uang C-M, Folz B. Posttensioned energy dissipating connections for moment resisting steel frames. *Journal of Structural Engineering* 2002; **128**(9):1111–1120. DOI: 10.1061/(ASCE)0733-9445(2002)128:9(1111)
- Ricles J, Sause R, Garlock M, Zhao C. Posttensioned seismic-resistant connections for steel frames. *Journal of Structural Engineering* 2001; **127**(2):113–121. DOI: 10.1061/(ASCE)0733-9445(2001)127:2(113)
- Rojas P, Ricles J, Sause R. Seismic performance of posttensioned steel moment resisting frames with friction devices. *Journal of Structural Engineering* 2005; **131**(4):529–540. DOI: 10.1061/(ASCE)0733-9445(2005)131:4(529)
- Garlock M, Sause R, Ricles J. Behavior and design of posttensioned steel frame systems. *Journal of Structural Engineering* 2007; **133**(3):389–399. DOI: 10.1061/(ASCE)0733-9445(2007)133:3(389)
- Kim H-J, Christopoulos C. Friction damped posttensioned self-centering steel moment-resisting frames. *Journal of Structural Engineering* 2008; **134**(11):1768–1779. DOI: 10.1061/(ASCE)0733-9445(2008)134:11(1768)
- Kurama YC, Sause R, Pessiki S, Lu L-W. Lateral load behavior and seismic design of unbonded post-tensioned precast concrete walls. *ACI Structural Journal* 1999; **96**(4):625–632.
- Toranzo LA, Restrepo JI, Mander JB, Carr AJ. Shake-table tests of confined-masonry rocking walls with supplementary hysteretic damping. *Journal of Earthquake Engineering* 2009; **13**(6):882–898. DOI: 10.1080/13632460802715040
- Midorikawa M, Azuhata T, Ishihara T, Matsuba Y, Matsushima Y, Wada A. Earthquake response reduction of buildings by rocking structural systems. *Smart Structures and Materials 2002: Smart Systems for Bridges, Structures, and Highways, Proceedings of SPIE*, San Diego, U.S.A., 2002. DOI: 10.1117/12.472562
- Palermo A, Pampinan S, Buchanan A. Experimental investigations on LVL seismic resistant wall and frame subassemblies. *Proceedings of the First European Conference on Earthquake Engineering and Seismology*, Geneva, Switzerland, 2006.
- Wiebe L, Christopoulos C, Tremblay R, Leclerc M. Shake table testing of a rocking steel frame designed to mitigate higher mode effects. *Behaviour of Steel Structures in Seismic Areas, Conference Proceedings*, Santiago, Chile, 2012; 703–708.
- Christopoulos C, Tremblay R, Kim H-J, Lacerte M. Self-centering energy dissipative bracing system for the seismic resistance of structure: development and validation. *Journal of Structural Engineering* 2008; **134**(1):96–107. DOI: 10.1061/(ASCE)0733-9445(2008)134:1(96)
- Tremblay R, Lacerte M, Christopoulos C. Seismic response of multistory buildings with self-centering energy dissipative steel braces. *Journal of Structural Engineering* 2008; **134**(1):108–120. DOI: 10.1061/(ASCE)0733-9445(2008)134:1(108)
- Kim H-J. Design of shake table test specimen. *Department of Civil Engineering Report*, University of Toronto, Toronto, ON, 2009.

20. American Society of Civil Engineers (ASCE). *Minimum Design Loads for Buildings and Other Structures, ANSI/SEI7-05 Including Supplement No.1*. American Society of Civil Engineers: Reston, Virginia, 2005.
21. American Institute of Steel Construction (AISC). *Load and Resistance Factor Design Specification for Structural Steel Buildings, ANSI/AISC 360-05 Including Supplement No.1*. American Institute of Steel Construction, Inc.: Chicago, Illinois, 2005.
22. American Institute of Steel Construction (AISC). *Seismic Provisions for Structural Steel Buildings, ANSI/AISC 341-05 Including Supplement No.1*. American Institute of Steel Construction, Inc.: Chicago, Illinois, 2005.
23. Christopoulos C, Filiatrault A, Folz B. Seismic response of self-centring hysteretic SDOF systems. *Earthquake Engineering and Structural Dynamics* 2002; **31**(5):1131–1150. DOI: 10.1002/eqe.152
24. Choi H, Erochko J, Christopoulos C, Tremblay R. Comparison of the seismic response of steel buildings incorporating self-centering energy-dissipative dampers, buckling restrained braces and moment resisting frames. *Report No. 05-2008*, Dept. of Civ. Eng., University of Toronto, Toronto, ON, 2008.
25. Tremblay R, Léger P, Rogers C, Bouaanani N, Massicotte B, Khaled A, Lamarche C-P. Experimental testing of large scale structural models and components using innovative shake table, dynamic, real-time hybrid simulation and multi-directional loading techniques. *Proceedings of the 3rd International Conference on Advances in Exp. Struct. Eng.*, San Francisco, USA, 2009.
26. McKenna F, Fenves GL, Scott MH, Jeremic B. *Open System for Earthquake Engineering Simulation (OpenSees) [Software]*. Pacific Earthquake Engineering Research Center, University of California: Berkeley, CA, 2000.
27. SelfCentering Material – OpenSeesWiki. Available from: http://opensees.berkeley.edu/wiki/index.php/SelfCentering_Material (accessed on 19 June 2012)
28. Computers and Structures Inc. *SAP 2000 [Software]*. Computers and Structures, Inc.: Berkeley, CA, 2009.
29. Le Bec A, Tremblay R, Erochko J, Christopoulos C. Modélisation du comportement d'une diagonale de contreventement SCED avec le logiciel d'analyse structurale SAP2000. *Rapport No. GRS SR10-02*, Département des génies civil, géologique et des mines, École Polytechnique de Montréal, Montreal, QC, 2010.
30. Erochko J. Improvements to the design and use of post-tensioned self-centering energy-dissipative (SCED) braces. *Doctoral Thesis*, University of Toronto, Toronto, Ontario, 2013.
31. Somerville P, Smith H, Puriyamurthala S, Sun J. Development of ground motion time histories for phase 2 of the FEMA/SAC steel project. *SAC Joint Venture, SAC/BD 97/04*, 1997.
32. Federal Emergency Management Agency. *FEMA-P695 Qualification of Building Seismic Performance Factors*. Federal Emergency Management Agency: Washington, DC, 2009.
33. Atkinson G. Earthquake time histories compatible with the 2005 NBCC uniform hazard spectrum. *Canadian Journal of Civil Engineering* 2009; **36**(6):991–1000.
34. American Institute of Steel Construction (AISC). *Code of Standard Practice for Steel Buildings and Bridges, ANSI/AISC 303-05*. American Institute of Steel Construction, Inc.: Chicago, Illinois, 2005.
35. Wiebe L, Christopoulos C. Characterizing acceleration spikes due to stiffness changes in nonlinear systems. *Earthquake Engineering and Structural Dynamics* 2010; **39**(14):1653–1670. DOI: 10.1002/eqe.1009
36. Wiebe L, Christopoulos C. Using Bézier curves to model gradual stiffness transitions in nonlinear elements: Application to self-centering systems. *Earthquake Engineering and Structural Dynamics* 2011; **40**:1535–1552. DOI: 10.1002/eqe.1099G